Rhinology, 43, 24-28, 2005

Numerical simulation of intranasal air flow and temperature after resection of the turbinates*

Joerg Lindemann[1], Tilman Keck[1], Kerstin M. Wiesmiller[1], Gerhard Rettinger[1], Hans-Juergen Brambs[2], Daniela Pless[2]

[1] Department of Otorhinolaryngology, University of Ulm, Ulm, Germany
[2] Department of Diagnostic Radiology, University of Ulm, Ulm, Germany

SUMMARY

***Background**: Radical surgical resection of the turbinates leads to a reduced intranasal air conditioning. The aim of this study was to determine the effect of turbinate resection on intranasal heating and airflow patterns using a numerical simulation.*

***Methods**: A bilateral model of the human nose with resection of the turbinates on one side based on a CT-scan was reconstructed. A numerical simulation applying the computational fluid dynamics (CFD) solver Fluent 6.1.22 was performed displaying inspiratory intranasal air temperature and airflow patterns.*

***Results**: Due to resection of the turbinates the airflow pattern is disturbed resulting in a spacious vortex throughout the entire nasal cavity. Hence, contact between air and surrounding nasal wall is less intense. Consequently, intranasal heating of the inspired air is relevantly reduced.*

***Conclusions**: Surgical resection of the turbinates leads to a disturbed intranasal air conditioning. The presented numerical simulation demonstrates the close relation between airflow patterns and heating.*

Key words: CFD, numerical simulation, turbinate resection, air conditioning, inspiration

INTRODUCTION

Climatization of the inspired air is the main function of the nose. In vivo intranasal humidity and temperature measurements were able to show that the turbinate complex and the lateral nasal wall mainly contribute to the heating and humidification of the inspired air [1, 2, 3].

The importance of the middle turbinate (MT) in nasal physiology is controversially discussed [4]. The MT plays an important role in humidification and heating of the incoming air, directing the inspiratory air stream towards the olfactory area. It protects the middle meatus from a turbulent airflow and supports mucociliary clearance. The MT plays a minor role in nasal resistance, being more attributed to the nasal valve area and the inferior turbinate (IT) [5, 6]. The turbinates dispose of a large mucosal surface as well as arteriovenous anastomoses and therefore distinctively contribute to nasal air conditioning [7]. The IT is primarily surgically treated for improvement of nasal obstruction caused by tissue hypertrophy. The MT represents an important landmark for endonasal sinus surgery and is mostly treated during sinus surgery in order to avoid postoperative adhesions to the lateral nasal wall.

Aggressive resection of the turbinates is supposed to disturb the balanced humidification and heating of the inspired air. As a consequence, reduced absolute humidity and temperature entail to common complaints like nasal dryness, crusting, fetor, recurrent nosebleed and hyposmia [8]. There still is a great lack of in vivo data about the influence of resection of the turbinates on nasal air conditioning [8]. In vivo temperature and humidity measurements within the entire human nose are technically and anatomically not realizable due to the complex anatomical structure of the nasal cavity. Therefore, in vivo measurements are not able to sufficiently display temperature and humidity distribution in high resolution.

Within this context, numerical simulations may play a helpful role in order to obtain more detailed information about nasal air conditioning after turbinate resection. As shown in previous studies, numerical simulations of intranasal airflow patterns and temperature distribution are feasible and provide detailed information about nasal air conditioning [9, 10]. The objective of this new study was to simulate intranasal air temperature and airflow distribution after turbinate resection during inspiration by means of computational fluid dynamics (CFD).

MATERIAL AND METHODS

Numerical simulation is a method able to reproduce a real

*Received for publication: April 26, 2004; accepted: July 19, 2004

environment within a computational model. CFD is a numerical simulation application to study fluid flow dynamics such as airflow patterns. In our study a computational model of the human nose with resected inferior and middle turbinate on the right side was reconstructed. The appropriate fluid flow physics were applied resulting in the calculation of expected inspiratory airflow patterns and temperature distribution within the model.

Model generation and meshing

A realistic three-dimensional (3D) model of the human nose was reconstructed from computed tomography (CT) scans of the nasal cavities of an adult male healthy volunteer. The CT scans were performed using a Philips Multislice CT Mx8000 (Philips Medical Systems, Eindhoven, the Netherlands). In the study presented coronary slices of 2 mm were applied allowing a more detailed geometry, whereas in previous studies a slice thickness of 3 mm for reconstruction of the nose models was used [10, 11]. The segmentation of the nasal cavity and the reconstruction of the surface model were achieved by employing the commercial segmentation software SURFdriver 3.5.6 (SURFdriver, Kailua, HW, USA). The segmentation was accomplished by slice-by-slice contour tracing. The left nasal cavity was segmented according to the anatomical morphology of the CT scan. Within the right nasal cavity the IT and MT were manually removed in each slice in order to simulate a surgical resection. After defining the contours of the nasal cavities, a surface model was generated. Smoothing was applied to the surface in order to avoid irregular edges disturbing the simulated airflow. The advantage of bilateral models over unilateral ones is the simultaneous display and comparison of airflow patterns as well as temperature distribution within the healthy nasal cavity as well as within the anatomically altered one. Processing of the model and application of the volume mesh was obtained by the commercial pre-processor Gambit 2.1.6 (Fluent Inc., Lebanon, NH, USA). In order to prevent unnecessary radiation exposure, the CT scan did not completely cover the nasopharyngeal region. For completion of the nose model, the nasopharynx had to be reconstructed using the Gambit modelling tool. The nasopharyngeal region is necessary for the accurate simulation of potential vortices within this area. Additionally, it was necessary to create the aperture of both nostrils as planar surfaces for computational purposes. Therefore, the model was cut with inclining symmetrical planes resulting in the openings of the nostrils. The nostrils represented the inflow areas, the terminating surface of the nasopharynx the outflow area of the model.

The complete model was provided with a volume mesh containing tetrahedron and hexahedron cells. Within the nasal cavities tetrahedron cells were employed, being refined in areas of small width such as the nasal valve area and the middle nasal meatus. In order to reduce the total number of cells and therefore computing time, hexahedron cells were used in the nasopharyngeal extension, resulting in a total of 360,000 cells for the entire model (Figure 1).

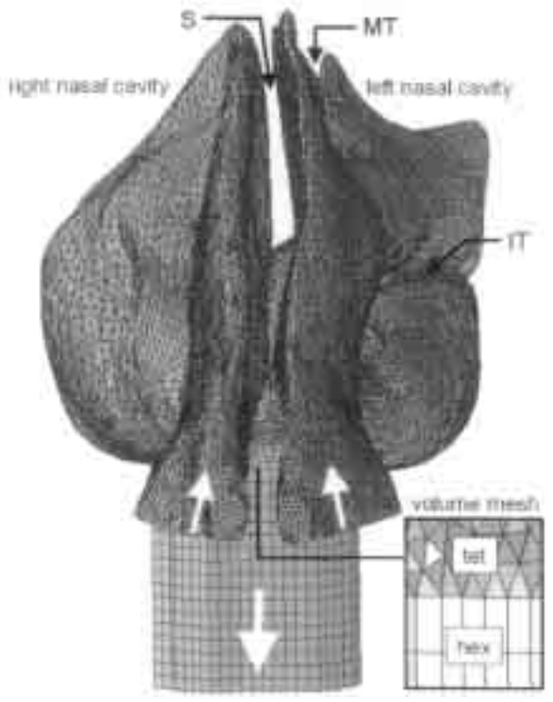

Figure 1. 3D-model of the nasal cavity (enlarged tetrahedron and hexahedron volume mesh) in frontal view (nasal septum (S), inferior turbinate (IT), middle turbinate (MT)). Inspiratory airflow direction is indicated by white arrows at the nostrils and the nasopharynx.

Numerical simulation

The numerical simulation was performed using the commercial CFD solver Fluent 6.1.22 (Fluent Inc., Lebanon, NH, USA). The simulation is based on the numerical solution of the Navier-Stokes equation representing the general equation for 3D flow of incompressible and viscous fluids. The RNG k-e turbulence model, a two-equation model, was applied in adaptation for turbulent flow of low Reynolds-numbers as given in the nasal airflow [11, 12]. The convergence of solution was controlled using the Fluent standard convergence criterions and special monitors.

The boundary conditions were defined as follows: the exterior wall of the model was assumed to be rigid. At the interface between air and surface of the nasal cavity the no-slip boundary condition was defined. Providing appropriate near-wall modelling, the enhanced wall treatment was selected. The simulation was performed for inspiration. In order to include the effects during the beginning of inspiration when the airflow is being accelerated, the simulation was carried out under unsteady conditions. The physiological air stream arising from negative pressure in the lungs was generated by a time-dependent negative pressure profile at the nasopharyngeal outflow in the numerical simulation (Figure 2). The pressure profile generates an acceleration of airflow at the beginning of inspiration to its maximum and a deceleration at the end of inspiration. The inspiratory cycle required 1.9 s, the pressure profile applied resulted in a flow profile according to a quiet respiration pattern (Figure 2)

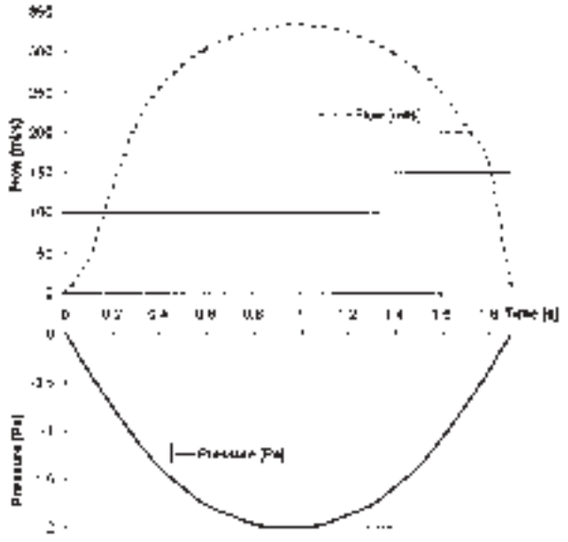

Figure 2. Pressure profile applied to the nasophyryngeal outflow generating the inspiratory airflow. The resulting flow curve is displayed according to quiet respiration pattern.

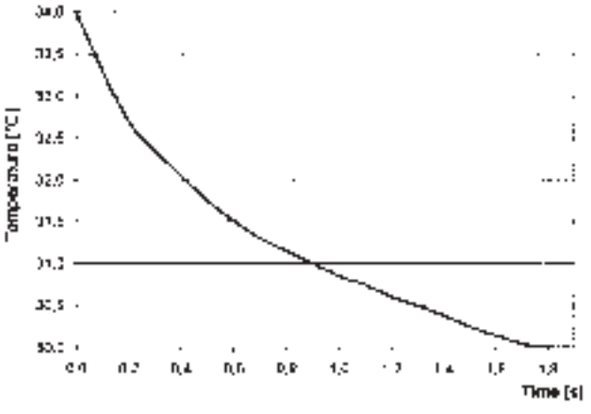

Figure 3. Temperature curve [°C] of the nasal wall during inspiration.

with a tidal volume of 470 ml. An initial air temperature of 20°C at the nostrils was assumed. According to our in vivo temperature measurements on the nasal mucosa [13, 14, 15], the nasal wall temperature was defined as time-dependent as well. A temperature curve decreasing from 34°C at the beginning to 30°C at the end of inspiration was used. In vivo, cooling of the nasal mucosa during inspiration is the consequence of heat transfer between inspired air and mucosa due to the temperature gradient. Since this particular heat exchange could not be simulated, the decrease in mucosal temperature over the period of inspiration was predefined as a temperature curve (Figure 3). Humidity and water exchange were not taken into consideration in this computational model. The numerical simulation included one inspiratory period (duration 1.9 s) representing a quiet breathing frequency of 14/min. For evaluation, intranasal air temperature distribution, air temperature adjacent to the wall as well as airflow patterns were displayed at the maximum flow rate during inspiration (t=1.0 s).

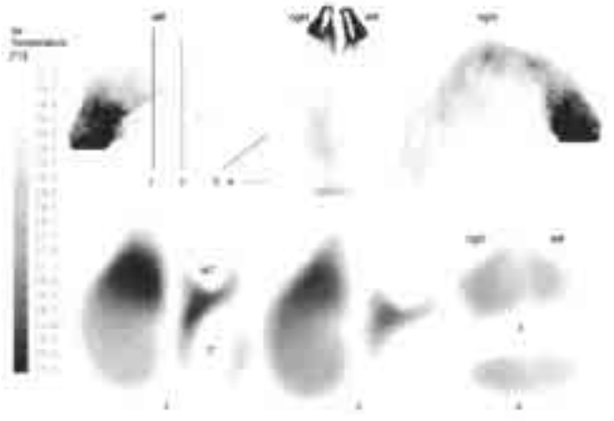

Figure 4. Air temperature distribution within the right and the left nasal cavity displayed as surface plot (upper row) and on cutting planes (1-4) as indicated.

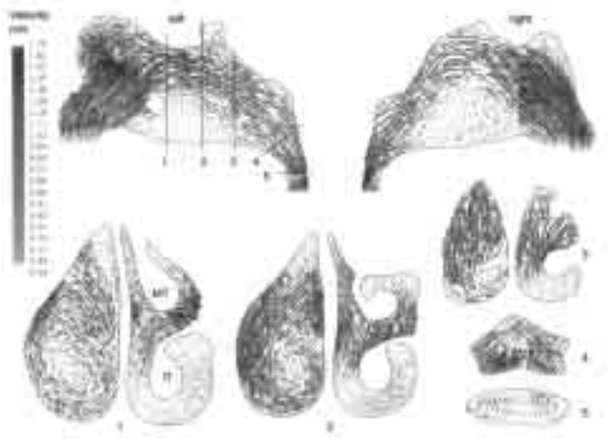

Figure 5. Airflow patterns as velocity vectors displayed on cutting planes through the left (left) and the right nasal cavity (right) and on cutting planes as indicated (1-5) (inferior turbinate (IT), middle turbinate (MT). The velocity magnitude is indicated by length of vectors and grey scaling.

RESULTS

A temperature plot was generated in order to evaluate the air temperature adjacent to the nasal wall. The intranasal air temperature was described by means of cutting planes across the nasal cavity. It was presented correspondingly to the gray scale on the left side of the figures. Black indicates low values; white represents high values (Figure 4). The airflow patterns were displayed as velocity vectors indicating flow direction as well as velocity magnitude. Long arrows represent high velocities, short ones low velocities (Figure 5).

During inspiration, in both nasal cavities the warm nasal wall is heating the inflowing cool air. Bilaterally, an increase in air temperature adjacent to the nasal wall could be detected within the entire nasal model (Figure 4).

Within the left nasal cavity, where turbinates remained untouched, more pronounced changes in air temperature could be

observed. An accentuated inspiratory increase in temperature within the centre of the air stream could be found in the anterior nasal segment posterior to the nasal valve area within the region of the IT and MT. The turbinates seem to be the main regions of heat exchange during inspiration.

Concerning air temperature distribution, a distinct difference could be observed between the intact left nasal cavity and the right one with the IT and MT removed. On the right side, pronounced changes in inspiratory air temperature could primarily be found adjacent to the nasal wall. At the original location of the turbinates, especially in the area of the IT, heating of the air decreased. The cool centre of the air stream on the right side increased compared to the left side where the turbinates remained untouched. The imbalanced air temperature distribution within the right nasal cavity extended into the nasopharyngeal region (Figure 4, cutting plane 1 to 4).

The comparison of airflow velocity (Figure 5) and air temperature reveals that areas of high increase in air temperature come along with low airflow velocities. On the other hand, minor changes in air temperature occur at high airflow velocities. The velocity distribution within the left nasal cavity shows that the areas of high increase in temperature, such as the region of the IT and MT, are characterized by a turbulent airflow of low velocities. The right nasal cavity provides a spacious vortex with its centre at the original position of the IT extending all over the nasal cavity and into the nasopharyngeal region (Figure 5, cutting plane 3). As a result, reduced blending of the air adjacent to the nasal wall with the air in the centre causing decreased heating of the inspiratory air can be observed. The determining factors influencing nasal airflow and temperature after turbinate resection seem to be the reduction of the nasal wall surface, changes of airflow patterns, and an enhancement of the nasal cavity volume due to turbinate resection.

DISCUSSION

In the literature, a multitude of techniques in turbinate surgery is described [16]. Various modalities of turbinate reduction procedures are available for treatment of chronic nasal obstruction due to hypertrophic IT [17, 18]. The MT may also be treated in numerous different ways from partial to total resection [5, 19]. In some authors' opinion a routine resection of the MT should be rejected due to the risk of anosmia, recurrent bleeding and atrophic rhinitis [20, 21]. Other authors propagate the resection of the MT without any disadvantages [22, 23, 24]. Additionally, different stabilization techniques to preserve the MT and to avoid lateral synechia seem to be popular [25, 26, 27, 28]. The vast number of techniques in turbinate surgery illustrates the problem of the ideal technique of interventional surgery.

The nasal turbinates were naturally developed to carry out certain functions including heating and humidification of the inspiratory air. The intention of surgical turbinate reduction should be the improvement of complaints while preserving their physiological function. Turbinectomy reduces nasal resistance, also causing an impaired respiratory function of the nose. The one major difficulty in turbinate surgery is a reduction of tissue resulting in an insufficient improvement of nasal obstruction on the one hand. On the other hand, a too excessive reduction of the turbinate entails desiccation and crusting.

In diverse in vivo measurements of intranasal air temperature and humidity we were able to demonstrate that in particular the turbinate complex and the lateral nasal wall mainly contribute to air conditioning [1, 2, 3]. Aggressive turbinate surgery significantly disturbs this process [8]. The study presented is the first attempt to simulate intranasal air temperature and airflow patterns during inspiration in a realistic human nose model after turbinate resection by means of a computational fluid dynamics (CFD) application.

Within the nasal cavity untouched, areas of low velocities with turbulences and vortices around the turbinates correspond with a distinct increase in air temperature during inspiration. The IT and MT remained the main regions of heat exchange. In contrast, within the altered nasal cavity one large static vortex develops, lacking any relevant flow towards the nasopharynx. As a consequence, a warm air layer adjacent to the nasal wall preventing from effective mixing and heating of the air within the centre of the air stream. Thus, relevant changes in air temperature had mainly been found adjacent to the nasal wall due to missing flow turbulences and the preponderance of laminar airflow. Due to the elongated vortex, reduced heating of the inspiratory air on the altered side could be found within the nasopharyngeal region.

The turbinates possess a large mucosal surface and essentially contribute to heating of the inspiratory air. A possible explanation of the relevantly reduced heat exchange between air and surrounding mucosa might be the loss of mucosal surface as heating source after to the turbinate resection. During inspiration, this loss of nasal tissue may lead to a reduced heat supply of the inspired air. During expiration the heat recovery from the warmed exhaled air might therefore also be negatively affected. In a theoretical model, blood temperature distribution along the airway wall, representing the nasal mucosal temperature, as well as the nasal cavity volume are considered to be the two main predictive factors for the effectiveness of nasal air conditioning [29]. These two parameters determine the local heat exchange within the upper respiratory system. Therefore, a reduction of nasal mucosal surface and the enhancement of the nasal volume cause a reduced heat exchange, creating a serious disparity between heat supply and demand.

Within the healthy nose, the inspired air passes the nasal valve area changing the laminar airflow into a turbulent one, allowing intensive contact between air and nasal mucosa. The respiratory air is spread all over the mucosal lining of the adjoining turbinate area in order to assure sufficient contact between air and mucosa. Turbulent airflow provides more kinetic energy than laminar airflow, hence, heat exchange between inspired air and nasal mucosa is more effective and intensive in areas of turbulences. The resection of the turbinates also causes an alternation within the nasal valve area. The resection of the anterior head of

the IT as part of the nasal valve area entails a less intense contact due to a more laminar airflow. In this case, the airflow is parallel to the nasal surface and exclusively air near to the mucosa comes into closer contact. In turbulent air flow with multiple small vortices, sideway motions occur, ensuring intensive contact between air and mucosa, creating best possible conditions for an appropriate heat exchange. Therefore, the regions of the turbinates seem to represent the actual functional part of the nose. It can be described as slit-like space allowing improved contact of air and mucosa [30]. Due to increased cross sectional areas and decreased airflow resistance after turbinate resection, the airflow remains more laminar and the contact of air and surrounding mucosa is less intensive. These facts demonstrate the close relation of airflow patterns and air conditioning in the human nose.

CONCLUSIONS

A CFD simulation of the intranasal air temperature and airflow patterns during inspiration in nose models with and without removal of the turbinates is feasible. Radical resection of the IT and MT disrupts the intranasal air conditioning due to disturbances of the airflow, loss of nasal mucosa and enlargement of the nasal cavity volume. The simulation presented demonstrates the close relation between airflow patterns and heating of inspired air. Since humidification is another important factor in air conditioning, our study group plans to analyze humidity distribution in CFD simulations.

ACKNOWLEDGMENT

The authors would like to thank Dr.-Ing. Ralf Kroeger from Fluent Deutschland GmbH (Darmstadt, Germany) for technical assistance.

REFERENCES

1. Keck T, Leiacker R, Heinrich A, Kühnemann S, Rettinger G (2000) Humidity and temperature profile in the nasal cavity. Rhinology 38: 167-171.
2. Lindemann J, Kuehnemann S, Stehmer V, Leiacker R, Rettinger G, Keck T (2001a) Temperature and humidity profile of the anterior nasal airways in patients with nasal septal perforation. Rhinology 39: 202-206.
3. Lindemann J, Leiacker R, Stehmer V, Rettinger G, Keck T (2001b) Intranasal temperature and humidity profile in patients with nasal septal perforation before and after surgical closure. Clin Otolaryngol 26: 433-437.
4. Kennedy DW (1998) Middle turbinate resection. Arch Otolaryngol Head Neck Surg 124: 107.
5. Courtiss EH, Goldwyn RM (1983) The effects of nasal surgery on airflow. Plast Reconstr Surg 72: 9-19.
6. Haight SJ, Cole PH (1983) The site and function of the nasal valve. Laryngoscope 93: 49-55.
7. Mygind N (1979) Applied physiology of the nose. In: Mygind N, editor. Nasal allergy. Oxford London Edinburgh Boston Melbourne: Blackwell Scientific Publications p 39-56.
8. Lindemann J, Leiacker R, Sikora T, Rettinger G, Keck T (2002a) Impact of unilateral sinus surgery with resection of the turbinates by means of midfacial degloving on nasal air conditioning. Laryngoscope 112: 2062-2066.
9. Lindemann J, Keck T, Wiesmiller K, Sander B, Brambs H-J, Rettinger G, Pless D (2004a) A numerical simulation of intranasal air temperature during inspiration. Laryngoscope 114: 1037-1041.
10. Pless D, Keck T, Wiesmiller K, Aschoff AJ, Fleiter TR, Lindemann J (2004) Numerical simulation of air temperature and airflow patterns in the human nose during expiration. Clin Otlaryngol (in press).
11. Keyhani K, Scherer PW, Mozell MM (1995) Numerical simulation of airflow in the human nasal cavity. J Biomech Eng 117: 429-441.
12. Bockholt U, Mlynski G, Muller W, Voss G (2000) Rhinosurgical therapy planning via endonasal airflow simulation. Comput Aided Surg 5: 175-179.
13. Lindemann J, Leiacker R, Wiesmiller K, Rettinger G, Keck T (2004b) Immediate effect of benzalkonium-chloride in decongestant nasal spray on the human nasal mucosal temperature. Clin Otolaryngol 29: 357-361.
14. Lindemann J, Leiacker R, Rettinger G, Keck T (2002b) The effect of topical xylometazoline on the mucosal temperature of the nasal septum. Am J Rhinol 16: 229-234.
15. Lindemann J, Leiacker R, Rettinger G, Keck T (2002c) Nasal mucosal temperature during respiration. Clin Otolaryngol 27: 135-139.
16. Clement WA, White PS (2001) Trends in turbinate surgery literature: a 35-year review. Clin Otolaryngol 26: 124-128.
17. Hol MK, Huizing EH (2000) Treatment of inferior turbinate pathology: a review and critical evaluation of the different techniques. Rhinology 38: 157-166.
18. Jackson LE, Koch RJ (1999) Controversies in the management of inferior turbinate hypertrophy: a comprehensive review. Plast Reconstr Surg 103: 300-312.
19. Giacchi RJ, Lebowitz RA, Jacobs JB (2000) Middle turbinate resection: issues and controversies. Am J Rhinol 14: 193-197.
20. Kennedy DW (1985) Functional endoscopic sinus surgery: technique. Arch Otolaryngol 3: 576-582.
21. Stammberger H (1991) Operative techniques. Chicago: WB Saunders Publisher p 290-296.
22. Biedlingmaier JF (1993) Endoscopic sinus surgery with middle turbinate resection: results and complications. Ear Nose Throat J 72: 351-355.
23. Cook PR, Begegni A (1995) Effect of partial middle turbinectomy on nasal airflow and resistance. Otolaryngol Head Neck Surg 113: 413-419.
24. Friedman M, Caldarelli DD, Venkatesan TK, Pandit R, Lee Y (1996) Endoscopic sinus surgery with partial middle turbinate resection: effects on olfaction. Laryngoscope 106: 977-981.
25. Bolger WE, Kuhn FA, Kennedy DW (1999) Middle turbinate stabilization after functional endoscopic sinus surgery: The controlled synechiae technique. Laryngoscope 109: 1852-1853.
26. Friedman M, Landsberg R, Tanyeri H (2000) Middle turbinate medialization and preservation in endoscopic sinus surgery. Otolaryngol Head Neck Surg 123: 76-80.
27. Lindemann J, Keck T, Rettinger G (2002d) Septal-turbinate-suture in endonasal sinus surgery. Rhinology 40: 92-94.
28. Hanna LM, Scherer PW (1986) A theoretical model of localized heat and water vapour transport in the human respiratory tract. J Biomec Eng 108: 19-27.
29. Thornton S (1996) Middle turbinate stabilisation technique in endoscopic sinus surgery. Arch Otolaryngol Head Neck Surg 122: 869-872.
30. Mlynski G, Grutzenmacher S, Plontke S, Mlynski B, Lang C (2001) Correlation of nasal morphology and respiratory function. Rhinology 39: 197-201.

Joerg Lindemann, MD
Department of Otorhinolaryngology, University of Ulm
Prittwitzstrasse 43
D- 89075 Ulm
Germany

Tel: +49-731-5003-3001
Fax: +49-731-5002-6703
E-mail: joerg.lindemann@medizin.uni-ulm.de